

Biomimetic Polysaccharide Nanocomposites of High Cellulose Content and High Toughness

Anna J. Svagan, My A. S. Azizi Samir, and Lars A. Berglund*

Royal Institute of Technology, Department of Fiber and Polymer Technology,
SE-100 44 Stockholm, Sweden

Received March 20, 2007; Revised Manuscript Received June 12, 2007

Plant cell walls combine mechanical stiffness, strength and toughness despite a highly hydrated state. Inspired by this, a nanostructured cellulose network is combined with an almost viscous polysaccharide matrix in the form of a 50/50 amylopectin–glycerol blend. Homogeneous films with a microfibrillated cellulose (MFC) nanofiber content in the range of 10–70 wt % are successfully cast. Characterization is carried out by dynamic mechanical analysis, field-emission scanning electron microscopy, X-ray diffraction, and mercury density measurements. The MFC is well dispersed and predominantly oriented random-in-the-plane. High tensile strength is combined with high modulus and very high work of fracture in the nanocomposite with 70 wt % MFC. The reasons for this interesting combination of properties include nanofiber and matrix properties, favorable nanofiber–matrix interaction, good dispersion, and the ability of the MFC network to maintain its integrity to a strain of at least 8%.

Introduction

Polysaccharides such as cellulose, chitin, and starch are widely available in nature and constitute an important class of biopolymers. They are extracted from renewable resources and may often be obtained at low cost. Starch can be obtained from roots, seeds, and stems from a variety of plants,¹ and is of commercial interest in packaging materials such as films and foams.² In the glassy state, starch tends to be brittle. For this reason, plasticized native starch is of interest as a thermoplastic biodegradable polymer matrix. Water and glycols are commonly used plasticizers, although urea and formamide have also been explored.³ An important limitation is that plasticized starch is sensitive to moisture and shows low strength. Two routes have been used to overcome these problems. The first is blending with biodegradable polymers such as polyhydrobutyrate,⁴ poly(lactic acid),⁵ polycaprolactone,⁶ and chitosan,⁷ and the second is preparing composites based on organic^{8,9} or inorganic^{10,11} reinforcement.

In plant cell walls, water is plasticizing the tissue, and yet the cell wall material combines mechanical stiffness and strength with toughness. Whitney et al. studied cellulosic nanocomposites in order to understand the function of the cellulosic network in the primary wall of plant cells.¹² The composites typically had a water content of 95% and still behaved as a solid material due to the cellulose microfibril network. An interesting possibility to improve starch properties is therefore to produce bioinspired nanocomposites through reinforcement of highly plasticized starch by microfibrillated cellulose (MFC) nanofibers. Polymer composites used commercially are usually combinations of petroleum-based synthetic polymers and strong fibers such as carbon, glass, aramide, or polyethylene. The bioinspiration in composites of MFC and starch is therefore expressed in several ways. Raw materials are from renewable resources, the fibrous reinforcement has nanoscale lateral dimension, and casting of composites takes place in water at ambient pressure and temperature.

Herrick et al.¹³ and Turbak et al.¹⁴ described a method for the preparation of MFC. Wood pulp fibers in a dilute water suspension were disintegrated into cellulose fibrils of nanoscale thickness in a homogenizer commonly used in the food industry. The aspect ratio (length/diameter) of MFC is very high, and a water suspension of 1 wt % MFC shows gel-like behavior. Depending on the plant source and the degree of disintegration, the MFC lateral dimension is typically in the range of 4–40 nm. The Young's modulus of the cellulose crystal is as high as 134 GPa.¹⁵ Since the typical tensile strength of microscale flax fiber cells approaches 1 GPa,¹⁶ the strength of nanoscale MFC has the potential to substantially exceed this value.

The term “microfibrillated cellulose” (MFC) refers to cellulosic fibrils disintegrated from the plant cell walls. MFC should not be confused with the term “microfibril” used in ultrastructural studies of cellulose and plant cell walls. Microfibrils are the 3–10 nm thick fibrils formed during cellulose biosynthesis in higher plants.¹⁷ The thickness of MFC could, in principle, be as small as 3–10 nm, but is typically in the range of 20–40 nm since it usually consists of aggregates of cellulose microfibrils. The structure of MFC is distinctly different from that of the low aspect ratio microcrystalline cellulose obtained by acid hydrolysis. We recently developed a new procedure to disintegrate MFC where a pretreatment procedure involving enzymes facilitates MFC disintegration.¹⁸ However, the mechanism by which the exposure of cellulose fibers to the endoglucanase enzyme facilitates disintegration is not fully understood.

The use of cellulose nanofibers in composite materials has recently been reviewed.^{19,20} Kubat et al.²¹ reported that cellulose nanocomposites based on a poly(vinyl acetate) matrix showed significantly improved mechanical properties compared with the matrix. Publications on cellulose whisker nanocomposites^{22,23} inspired more recent activities. Cellulose whiskers with an aspect ratio of around 100 were disintegrated from tunicate mantles.²⁰ Strong reinforcement effects were demonstrated for nanocomposites based on up to 10 wt % of cellulosic tunicin whiskers.^{20,23} The reinforcement effect was particularly strong with the matrix in the rubbery state. The mechanism for reinforcement

* Corresponding author. E-mail address: blund@kth.se.

was through the stiffening effect provided by a network of tunicin whiskers formed during the composite film casting process. Tunicin whisker nanocomposites are well suited as model materials. The whiskers are discrete and rod-like, and the approximate range of whisker aspect ratios may be characterized experimentally. Cellulose microfibrils of well-defined and uniform structure are also produced by bacteria,²⁴ although bacterial cellulose is currently too expensive for uses other than in specific high-technology applications.

Wood-based MFC is potentially of commercial interest since the cost may be quite low. Nakagaito and Yano combined cellulosic pulp fiber-based MFC networks from wood with a small amount of phenol-formaldehyde resin matrix to produce high-strength composites.²⁵ Yano and Nakahara produced MFC materials with a modulus of 16 GPa using MFC only.²⁶ As Yano and Nakahara added 2 wt % starch to their MFC films, strength increased although modulus decreased significantly (from 16 to 12.5 GPa). A limitation with the mentioned materials is very low strain-to-failure.

In the present study, the objective is to first prepare MFC nanocomposites with a plasticized matrix, and then study relationships between structure and mechanical properties. MFC content is the main structural parameter of variation. Efforts are directed toward high MFC volume fraction nanocomposites with a ductile amylopectin matrix. This is in order to search for bioinspired nanocomposites combining modulus and strength with high work of fracture (toughness). Two previous studies are related to the present work, although interesting failure properties are not reported or discussed. Dufresne and Vignon²⁷ focused on the effects of potato-based MFC on the modulus of non-plasticized starch nanocomposites. López et al.²⁸ used MFC similar to that used in the present study, although the MFC content was significantly lower. In both studies, the materials contained moisture. This is probably motivated by the importance of moisture during the practical use of starch composites. However, the interpretation of structure–property relationships becomes more difficult, and this is why the majority of the present data are from dry nanocomposites.

Experimental

Materials. Granular amylopectin potato starch with an amylose content lower than 1 wt % was kindly supplied by Lyckeby Stärkelsen (Kristianstad, Sweden). MFC in a 2 wt % water suspension was kindly supplied by professor Tom Lindström at STFI-Packforsk AB in Stockholm, Sweden. The preparation of MFC is described in detail elsewhere.^{18,29} Bleached sulfite softwood cellulose pulp (Domsjö ECO Bright; Domsjö Fabriker AB) consisting of 40% pine (*Pinus sylvestris*) and 60% spruce (*Picea abies*) with a hemicellulose content of 13.8% and a lignin content of 1% was used as a source for the MFC. The pulp was used in its never-dried form. The cell wall delamination was carried out by treating the sulfite pulp in four steps: a refining step in order to increase the accessibility of the cell wall to the subsequent monocomponent endoglucanase treatment, an enzymatic treatment step, a second refining stage, and finally a process in which the pulp slurry is passed through a high-pressure homogenizer. A microbicide (5-chloro-2-ethyl-4-isothiazolin-3-one) was also added to the MFC in order to avoid bacterial growth. The weight-average molecular weight (M_w) of the cellulose in the MFC is 200 000 g/mol. Glycerol (99% GC) and drying agent (silica gel, SiO₂) were purchased from Sigma-Aldrich.

Preparation of Films. The amylopectin starch was dispersed in deionized water (3 wt %) and gelatinized by heating to 65 °C and maintaining this temperature for less than 5 min in a closed E-flask during magnetic stirring. The formed gel was then heated for another 120 min in an oil bath in a closed steel cylinder on a rotating rack.

The interior of the cylinder was kept at 135 °C. The pregelatinization was performed in order to ensure good mixing. The solution obtained was optically transparent and less viscous than before.

The MFC suspension and glycerol were added in varying amounts to the obtained amylopectin solution. The cellulose content was varied from 0 to 70 wt % (MFC/(amylopectin + glycerol + MFC)), and the glycerol content was varied from 0 to 50 wt % (glycerol/(amylopectin + glycerol)). Neat and plasticized MFC films were prepared by diluting the 2 wt % MFC suspension to ~1.3 wt % and adding glycerol; 0–60 wt % (glycerol/(glycerol + MFC)). The new suspensions were magnetically stirred for 6 days at room temperature, and, after 3 days, suspensions containing MFC were mixed (8000 rpm) using an Ultra Turrax mixer (IKA, DI25 Basic) for 15 min. The suspensions were degassed and cast in Teflon-coated petri dishes. All plates, except the neat and plasticized MFC plates, were dried in a sterile ventilated oven at 30 °C without forced air-flow, until they appeared dry. The MFC plates were dried at room temperature. Films were cut into specimens and dried for 2 days in a vacuum oven at 40 °C or conditioned at 50% relative humidity (RH) and 23 °C for at least one week. Prior to testing, the dry specimens were stored in a desiccator with drying agent.

Thermogravimetric Analysis (TGA). TGA was used to determine the water content of the films conditioned at 50% RH and 23 °C. A Mettler Toledo (TGA/SDTA 851^e) thermal gravimetric analyzer was used. About 10 mg of the sample was heated from 35 to 105 °C at a rate of 5 °C/min, followed by an isothermal step at 105 °C for 30 min. The nitrogen flow was 50 mL/min. The water content was calculated by dividing the weight loss by the initial weight of the sample. The water content was averaged over three measurements.

Field-Emission Scanning Electron Microscopy (FE-SEM). For micro-structural analysis, the films were observed by FE-SEM. The specimens were first frozen in liquid nitrogen and then fractured. They were fixed on a metal stub using carbon tape and coated with gold using an Agar HR sputter coater. A Hitachi s-4300 scanning electron microscope operating at 2 kV was used to obtain the secondary electron images.

X-ray Diffraction. Diffractograms were recorded in reflection mode in the angular range of 4–40° (2 θ) by steps of 0.05°. The measurements were done with a X'Pert Pro diffractometer (model PW 3040/60). The CuK α radiation (1.5418 Å) generated at 45 kV and 40 mA was monochromatized using a 20 μ m Ni filter. Diffractograms were recorded from rotating specimens (revolution time 8 s) using a position-sensitive detector (X'Celerator detector). The scanning speed was 0.0318° s⁻¹, and the total scanning time was 20 min for each specimen.

Dynamic Mechanical Analysis (DMA). A Q800 TA Instruments DMA operating in tensile mode was used. Rectangular strips (approximately 20 × 5 × 0.2 mm) were cut from the films and dried for 2 days in a vacuum oven at 40 °C. The measurement frequency and strain were 1 Hz and 0.05%, respectively. The specimens were mounted and then dried for 10 min at 100 °C in the DMA to remove any residual moisture in the specimen and then cooled down and equilibrated at –96 °C. The specimens without MFC could not be dried at 100 °C in the DMA, because they cracked at 100 °C. These specimens were immediately cooled to –96 °C. The measurements were made at a heating rate of 3 °C/min. The attained storage modulus values were normalized at 23 or 21 °C (specimens tested on Minimat) to the mean modulus values obtained from tensile testing.

Tensile Test. The tensile testing was performed on an Instron 5567 universal testing machine, equipped with a load cell of 500 N and on a Miniature Materials Tester 2000 (Minimat) with a load cell of 20 N. The films were cut in thin rectangular strips: 5 mm wide and at least 60 mm long and about 0.2 mm thick, except for two films where shorter lengths were selected in order to obtain homogeneous thickness. The gauge length was 40 mm for the long samples and 30 mm for the shorter samples. The strain rate was 10% min⁻¹. The tensile test on the Instron machine was performed at 50% RH and 23 °C, while the testing with the Minimat was performed at ambient conditions (21 °C and ~38% RH). When testing dry samples, sample dimension measurements,

Table 1. Glass Transition Temperatures of Amylopectin–Glycerol Films with Varying Glycerol Content

glycerol (wt %)	DMA	
	$T_g^l(^{\circ}\text{C})^a$	$T_g^u(^{\circ}\text{C})^b$
0	nd ^c	nd
17	−38	161
29	−38	102
42		
50	−45	7

^a The lower glass transition temperature. ^b The upper glass transition temperature. ^c nd = not detected.

mounting of the sample, and tensile testing were done in the quickest possible way to minimize water absorption and were, in all cases except for one material, performed within 10 min. The testing of the plasticized amylopectin material with 50 wt % glycerol was performed within 15 min on the Minimat. Under these testing conditions, the moisture absorption is low and the samples are considered dry throughout the testing.

Stress–strain curves were plotted, and the Young's modulus was determined from the slope of the low strain region. The work of fracture, strength, and strain-to-failure were also determined for each specimen. The work of fracture corresponds to the area below the stress–strain curve. Mechanical tensile data were averaged over at least three specimens.

Density. The volume of the material was measured by a mercury displacement apparatus,³⁰ which works according to Archimedes principle. The sample is weighed in air, m_1 , and when submerged in mercury, m_2 . The buoyancy of the sample is thus obtained and thereby the sample volume:

$$V_{\text{sample}} = \frac{m_1 - m_2}{\rho_{\text{Hg}} - \rho_{\text{air}}} \approx \frac{m_1 - m_2}{\rho_{\text{Hg}}}$$

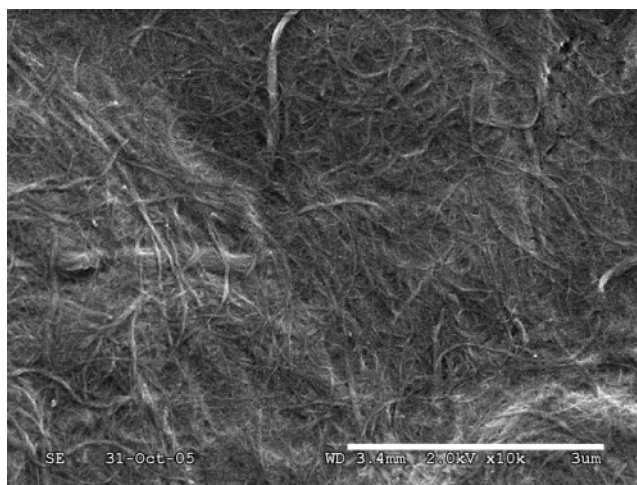
The density of the material is obtained by dividing the mass of the sample in air by the volume of the sample. The sample dimensions were 2×3 cm, and the density obtained was an average over two vacuum-dried test specimens.

Results and Discussion

The cellulose nanocomposites in the present study contain wood-based MFC reinforcement in a matrix of amylopectin plasticized by glycerol. In order to avoid the complexity of water as an additional constituent in the system, data are from dry specimens unless stated otherwise. Glycerol serves as an amylopectin plasticizer. However, in the context of plant cell walls as inspiration for new materials, glycerol is also an experimentally convenient substitute for water as a plasticizer since the glycerol vapor pressure at a given temperature is lower.

Plasticized Amylopectin Matrix. *Dynamic Mechanical Behavior.* In order to have a highly ductile matrix, the glycerol content in the plasticized amylopectin matrix is selected such that the matrix is above the glass transition temperature T_g at room temperature. Table 1 provides the upper and lower glass transition temperatures obtained by DMA for amylopectin–glycerol films with different compositions.

For all samples there is a weak mechanical relaxation process at about -45 or -38°C , indicated by a drop in storage modulus and a peak in $\tan \delta$. At higher temperatures a stronger mechanical relaxation is observed for the plasticized films. The lower temperature transition shows a weak dependence on composition, whereas the high-temperature relaxation decreases in temperature with increased glycerol content. Also, the storage modulus decreases more rapidly with temperature as the glycerol

**Figure 1.** FE-SEM micrographs of a cellulose nanocomposite film surface, 50 wt % MFC, 50/50 amylopectin/glycerol matrix. The scale bar is $3 \mu\text{m}$.

content is increased (not shown here). The T_g of the dry unplasticized amylopectin film was not detectable by DMA, because it is above the degradation temperature of starch.

Many authors have reported starch and glycerol to be only partially miscible.^{31–33} This results in a phase-separated system of starch-rich and glycerol-rich domains. Moates et al.³³ argued that the lower transition of glycerol-plasticized amylose films was an α -relaxation process and estimated its activation energy for different mixtures of glycerol–amylose. They found support for the argument in that the activation energy was comparable to that of pure glycerol. Thus, the low-temperature relaxation is the glass transition of a glycerol-rich amylopectin region. The relaxation at high temperature is the T_g of the starch-rich region. The starch-rich region^{31–33} is defined as a region containing mostly amylopectin but also glycerol.

The storage modulus of the plasticized amylopectin films can be tailored by altering the glycerol content (not shown here). The 50/50 mixture shows steeply decreasing modulus with temperature, and was selected as the major matrix composition. This is inspired by the viscous characteristics of the water–pectin matrix in a primary cell wall,¹² where the presence of a network based on cellulose microfibrils causes a favorable combination of modulus, strength, and ductility. It is then interesting to investigate the mechanical property improvement of a 50/50 amylopectin/glycerol mixture as MFC is added.

Structure of Films. *FE-SEM.* In Figure 1, a micrograph of a 50 wt % MFC nanocomposite film surface is presented. The random nature of the orientation distribution of the MFC is apparent. Some larger fibrous entities are present with a width of around 150 nm , and are cell wall fragments. In the context of mechanical performance, they must be considered defects. The presence of some porosity can be suspected on the basis of the micrograph. The width of most individual MFCs is estimated to be $30 \pm 10 \text{ nm}$, although wider fibrils are present. The length is several micrometers. The preparation and characteristics of MFC have been described in previous studies.^{18,29}

For MFC contents higher than 10 wt %, a lamellar organization of MFC is apparent (see Figure 2 a,b). The cryo-fractured surface in Figure 2a shows fibrous lamellae protruding from the surface, although individual MFC dots are also observable. Figure 2b illustrates regions of layered structures protruding from the fractured surface. The appearance is a result of the fracture mechanism and the MFC organization. The fracture surface indicates that the intralaminar MFC interaction is

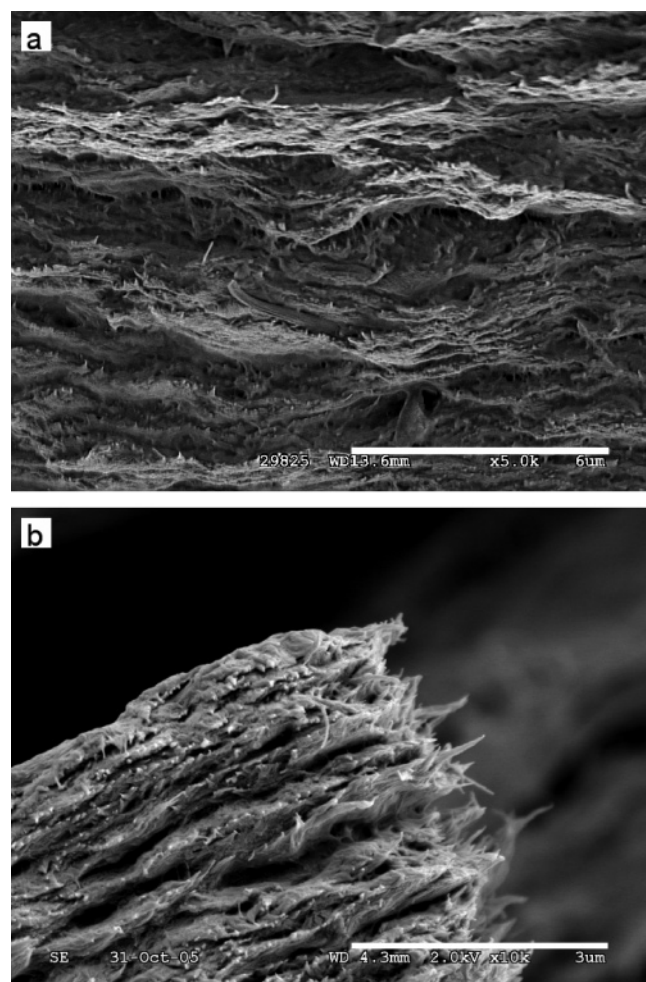


Figure 2. FE-SEM micrographs of cellulose nanocomposite films, 50/50 amylopectin/glycerol matrix: (a) 50 wt % MFC, freeze fractured; (b) 50 wt % MFC, fracture surface from tensile test. The scale bars are (a) 6 μm and (b) 3 μm .

stronger than the interlaminar one. This is a consequence of the random-in-the-plane orientation distribution of MFC.

It was possible to produce high cellulose content nanocomposites since the interaction is favorable between the constituents. In many other systems of MFC and water soluble polymers, the maximum MFC content is below 20 wt % and limited by MFC agglomeration. The micrographs in Figures 1 and 2, particularly the even distribution of the white dots representing fractured MFC, supports homogeneous MFC distribution in the matrix. This, along with the small MFC diameter, is important during deformation since localized failure events are delayed to higher strains.

Density. The density increases with MFC content, and is in the range of 1230–1300 kg/m^3 . The densities of neat plasticized and unplasticized matrix are 1210 and 1260 kg/m^3 , respectively. The lowest density is obtained for the neat MFC film (1140 kg/m^3), and this low value means that the film is porous.

The void content influences the properties of nanocomposites. Assuming that the theoretical densities of cellulose, amylopectin, and plasticized amylopectin are 1500, 1260, and 1210 kg/m^3 , respectively, we may calculate the theoretical density of the composites and also the void content, V_v :

$$V_v = \frac{\rho_{\text{ct}} - \rho_{\text{ce}}}{\rho_{\text{ct}}} \times 100$$

Table 2. Calculated Void Content of MFC–Amylopectin–(Glycerol) Composites

MFC (wt %)	void content (%)	
	plasticized starch matrix ^a	unplasticized starch matrix
10	0.3	
30	4.7	
40		3.9
50	8.0	
70	7.3	
100	24	

^a Fixed matrix composition with 50 wt % glycerol and 50 wt % amylopectin.

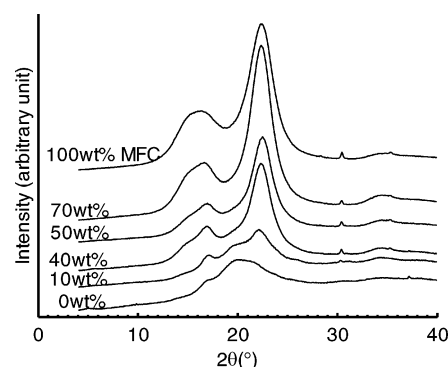


Figure 3. Diffractograms of films composed of varying amounts of MFC and fixed matrix composition (50 wt % glycerol and 50 wt % amylopectin). The MFC contents are indicated in the figure.

where ρ_{ct} and ρ_{ce} are the theoretical and experimental densities, respectively. The theoretical density of a composite is calculated from the densities of its constituents and their weight fractions.³⁴

Table 2 shows the calculated void content of different MFC nanocomposites. The neat MFC film has the largest void content at 24%. It is therefore a porous MFC network rather than a solid material. With higher void content, the fibril–fibril contact areas become smaller, and lower modulus is expected. Utilizing high pressure, Yano et al.²⁶ prepared hot-pressed MFC films with a density of 1480 kg/m^3 (about 1.3% void space) and a Young's modulus of 16 GPa determined in bending. This can be compared with the air-dried MFC film in the present paper with a Young's modulus and density of 13 GPa and 1140 kg/m^3 , respectively.

In the present case, the matrix fills the void space during MFC network formation. This gives a lower void content in composites compared to the neat MFC film (see Table 2). Voids have a negative influence on the stress transfer between MFC and the matrix. At higher void contents, this will significantly influence the elastic moduli of the composites. Failure properties such as strength and fatigue life will be even more sensitive to voids, since voids initiate failure. In the case of glass fiber and carbon fiber microcomposites, a void content of less than 1% is recommended.³⁴ However, those materials are based on brittle matrices and the present material is likely to be less void sensitive. In addition, the present void size is very small and smaller voids require higher stress in order to initiate failure.

X-ray Diffraction. X-ray diffractograms were collected from dry neat matrix (50/50 amylopectin/glycerol) and composite films with different MFC contents (see Figure 3). In dry conditions, the diffractogram of the neat matrix displays a broad hump and no diffraction peaks (but a shoulder at around 17.2°), characteristic of an amorphous material. Two peaks are observed for the dry composite films. The high peak at $\sim 22.5^\circ$ is due to the crystalline parts of MFC and is a characteristic of cellulose

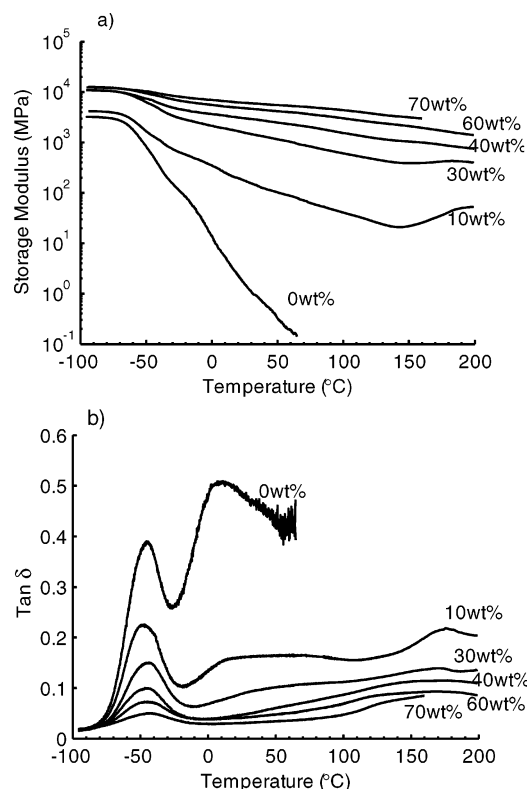


Figure 4. (a) Storage tensile modulus and (b) $\tan \delta$ curves of MFC–amylopectin–glycerol composites with fixed matrix composition (50 wt % glycerol and amylopectin) and varying MFC content. The MFC content is indicated in the figure.

I.³⁵ Another peak around 17.0° is observed for the materials containing 10, 40, and 50 wt % MFC. Since matrix transcrystallinity in the fiber–matrix interphase has been discussed in amylopectin–cellulose systems,³¹ this peak needs further analysis. The diffractograms of pure MFC and pure glycerol–amylopectin were combined by a simple rule-of-mixtures approach to create theoretical diffractograms for the MFC–glycerol–amylopectin composites. In the theoretical diffractograms (not shown here), the peak at around 17.0° also appears for the materials with 10, 40, and 50 wt % MFC contents. As a consequence, the peak is not associated with amylopectin, and we have no data in support of crystalline order or transcrystallinity in the matrix.

Helbert et al.³⁶ obtained oriented growth of V amylose *n*-butanol crystals on tunicate whiskers. This was achieved by seeding the solutions of amylose with tunicate whiskers. However, amylopectin is known to crystallize slowly. Rindlav–Westling et al.³⁷ reported that the development of crystallinity in amylopectin films was only possible in the presence of larger amounts of plasticizer (both glycerol and water) than that used in the present system.

MFC Reinforced Plasticized Amylopectin Composites. Dynamic Mechanical Behavior. Neat MFC films were studied by DMA (data not shown). Compared with the starch/glycerol matrix, the storage modulus is about 8000 times higher at 23°C . The temperature dependence of the modulus is fairly weak throughout the measured range of temperatures. The modulus decreases from around 18 to 7.3 GPa in the temperature interval of -96 to 200°C .

Figure 4 shows storage modulus and $\tan \delta$ as a function of temperature for MFC-reinforced plasticized amylopectin in the dry state with MFC contents from 0 to 70 wt %. At low temperatures, the storage modulus is almost constant with

increasing temperature. Compared with the plasticized amylopectin (50/50), the storage modulus of nanocomposites is much higher over the entire temperature range and decreases less rapidly with temperature. One relaxation transition is observed for all nanocomposites at low temperature. The transition temperature is the same as that observed for glycerol-rich regions in plasticized amylopectin. As further confirmation of peak origin, the height of the $\tan \delta$ peaks decreases with decreasing plasticizer content.

The $\tan \delta$ peak of the starch-rich region at 7°C observed for the plasticized amylopectin cannot be observed for the nanocomposites, although traces of this peak are discernible for the 10 wt % nanocomposite. The loss of the starch-rich region peak may indicate strong amylopectin–MFC interaction and the fact that MFC is restricting the molecular mobility of amylopectin.³⁸ The upper increase in $\tan \delta$ for the 10 wt % MFC nanocomposite is due to glycerol evaporation and increased storage modulus.

An important reinforcement effect from MFC is increased thermal stability of the modulus in the temperature interval of -96 to 200°C . At 23°C , the storage modulus is about 100 and 4000 times higher than the matrix at 10 wt % MFC and 70 wt % MFC, respectively. This is explained by the formation of an MFC network^{39–42} during the evaporation of water in the film preparation stage. Nair et al. prepared chitin whisker-reinforced natural rubber nanocomposites and found that the swelling behavior of the nanocomposites and the reinforcing effect of whiskers strongly depended on the ability of whiskers to form a network.^{40,41} Chemical modification of the surface of chitin whiskers was performed in order to improve interfacial adhesion between chitin and matrix.⁴² Despite the improved adhesion, the mechanical properties and thermal stability were found to be inferior to nanocomposites based on unmodified whiskers. This was ascribed to partial destruction of the three-dimensional whisker network.

In Figure 5, storage modulus and $\tan \delta$ are presented as a function of temperature for MFC-reinforced plasticized amylopectin films with 40 wt % MFC and varying glycerol contents in the matrix: 0, 29, and 50 wt % glycerol. Increased glycerol content leads to decreased modulus and a faster decrease in modulus with temperature. Again, only the low-temperature $\tan \delta$ peaks can be observed. The low-temperature peak of nanocomposites containing glycerol is due to the glycerol-rich amylopectin region. For the nanocomposite where the matrix does not contain glycerol, the peak is at similar position and is stronger than that of the corresponding neat MFC film and neat amylopectin peaks, which are due to a secondary relaxation process.⁴³ Montès et al.^{44,45} investigated secondary mechanical relaxation processes in amorphous cellulose and found them to be of an origin similar to that found in starch and other polysaccharides. Therefore, the secondary relaxation observed at -38°C for the unplasticized composite film is most likely associated with the added contribution from localized motions of the chain backbones of the MFC and amylopectin constituents. The peak observed at high temperature for a nanocomposite with a matrix containing 29 wt % glycerol is due to glycerol evaporation.

The results presented in Figure 5 demonstrate the possibility to control the storage modulus by changes in the glycerol content of the matrix. In addition, MFC content may be changed (see Figure 4) in order to provide additional tailoring possibilities.

Tensile Testing. In Figure 6, typical stress–strain curves are presented for MFC nanocomposites with plasticized matrix (50/50 amylopectin/glycerol). Average values of the mechanical properties are reported in Table 3. The most important result is

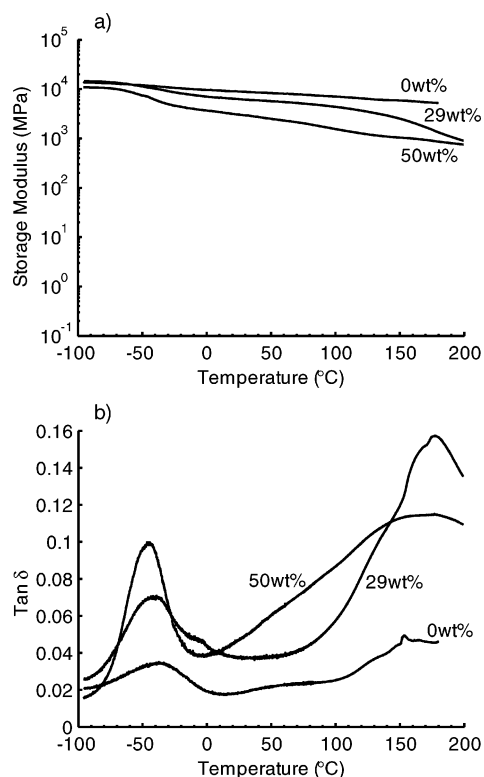


Figure 5. (a) Storage tensile modulus and (b) $\tan \delta$ curves of MFC–amylopectin–glycerol composites with 40 wt % MFC content and varying matrix composition. The glycerol contents in the matrix (glycerol/(glycerol + amylopectin)) are specified in the figure.

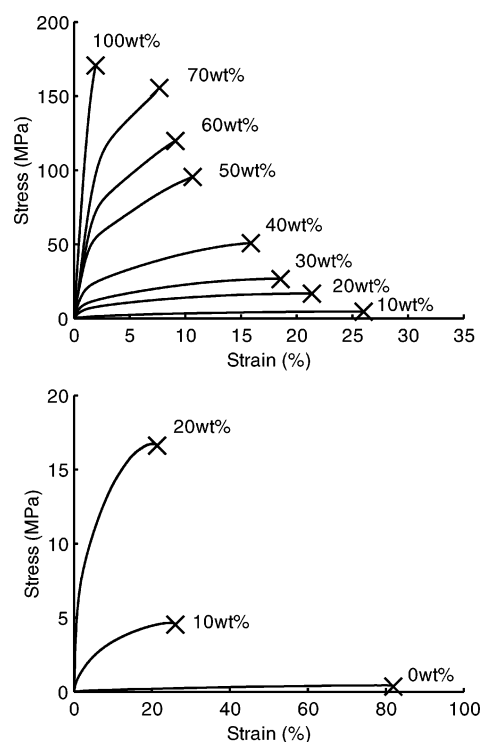


Figure 6. Typical tensile curves for MFC–amylopectin–glycerol composites with varying MFC content and fixed matrix composition: 50 wt % glycerol and 50 wt % amylopectin. The MFC contents are indicated in the figure.

that, at high MFC contents, the material combines high strength and modulus with high strain-to-failure. At a fibril content of 70 wt %, the modulus is 6.2 GPa, the strength is 160 MPa, and the strain-to-failure is 8.1%. The work of fracture is 9.4 MJ/

Table 3. Mechanical Properties of Composites with Fixed Matrix Composition (50 wt % Glycerol and 50 wt % Amylopectin) and Varying MFC Content^a

MFC (wt %)	Young's modulus (MPa)	tensile strength (MPa)	strain-to-failure (%)	work of fracture (MJ/m ³)
0 ^b	1.6 (0.88)	0.35 (0.05)	80 (9.5)	0.18 (0.04)
10	180 (23)	5.0 (0.20)	25 (0.93)	0.94 (0.05)
20	780 (100)	15 (1.5)	22 (0.88)	2.7 (0.22)
30	1600 (140)	31 (2.5)	18 (0.74)	4.0 (0.22)
40	3100 (90)	58 (5.0)	15 (0.98)	6.2 (0.38)
50	4300 (120)	80 (3.1)	11 (0.65)	6.5 (0.78)
60	4800 (190)	120 (5.5)	9.3 (0.52)	7.8 (0.49)
70 ^c	6200 (240)	160 (7.9)	8.1 (0.93)	9.4 (1.5)
100	13000 (1000)	180 (7.8)	2.1 (0.38)	2.4 (0.60)

^a The values in parentheses are the sample standard deviations.

^b Tensile testing done on a Miniature Material Tester. ^c All samples broke at grips.

m³, and this is remarkably high. As the MFC content increases, the Young's modulus and the strength both increase while the strain-to-failure decreases. It is notable that the trends in property changes with MFC content are quite consistent. This further indicates good dispersion of MFC and homogeneous character of the nanocomposites. The large increase in mechanical properties with MFC content is primarily due to the MFC network and the inherent properties of the MFC. Favorable interactions between MFC and the matrix is also a positive factor.^{27,38,39}

In the elastic range, elastic stretching of the MFC network is expected to dominate as the deformation mechanism. The onset of nonlinear deformation is related to the reorganization of the MFC network, perhaps by individual fibrils debonding from each other. The strong strain-hardening tendency in the post-yield region indicates some reorientation of the MFC. It is plausible that individual MFC fibrils start to fracture toward the end of the deformation process. Fracture surfaces do not show long pull-out lengths of individual fibrils (see Figure 2b).

Conventional microfiber composite materials such as glass fiber-reinforced thermoplastics (i.e., polypropylene, polyamide 6,6) may show high strength and modulus.^{46,47} However, the strain-to-failure is typically only around 2%. The interesting combination of mechanical properties in the present nanocomposites is due to the nanoscale of the fibrils, and the unique characteristics provided by the MFC network. It allows the use of a matrix with highly viscous properties. The small scale of fibril diameter is an advantage as fibril–matrix separation eventually takes place, since the scale of the separation length is about 3 orders of magnitude smaller than that for a microfiber composite.

In terms of mechanical performance, Dufresne and Vignon²⁷ primarily discussed the modulus in potato MFC-reinforced starch composites containing water and glycerol. Comparable data in the present study are much higher, and there may be two main reasons for this. In the present study, glycerol alone acts as a plasticizer of the amylopectin matrix. This may provide more favorable matrix stress transfer than the combination of water and glycerol in the materials studied by Dufresne and Vignon. Even if the total amount of plasticizer is the same, it is possible that the presence of water lowers interfacial adhesion more than glycerol does. Observations of the mechanical properties of the conditioned 50 wt % MFC nanocomposite with 50/50 amylopectin/glycerol matrix in Table 4 provide support for this explanation. The decrease in modulus and strength compared to that of the dry 50 wt % MFC composite in Table 3 is because

Table 4. Mechanical Properties of Composites with Fixed MFC Content and Varying Matrix Composition, MFC–Glycerol Films, and One Conditioned Composite with a (50/50) Amylopectin/Glycerol Matrix (Dry Weight Basis)^a

	Young's modulus (MPa)	tensile strength (MPa)	strain-to-failure (%)	work of fracture (MJ/m ³)
glycerol (wt %)	films with fixed MFC content (40 wt %)			
0	9000 (490)	150 (19) ^b	2.4 (0.34) ^b	2.1 (0.68) ^b
29	6300 (170)	130 (4.3)	5.9 (1.2)	5.3 (1.2)
42	3800 (230)	75 (3.0)	9.5 (0.90)	5.3 (0.77)
50	3100 (90)	58 (5.0)	15 (0.98)	6.2 (0.38)
glycerol (wt %)	MFC–glycerol films			
0	13000 (1000)	180 (7.8)	2.1 (0.38)	2.4 (0.60)
33	2600 (180)	44 (0.8)	9.3 (0.76)	2.9 (0.25)
60	240 (55)	4.7 (1.6)	10 (1.9)	0.34 (0.06)
MFC (wt %)	conditioned composite film			
50 ^c	1700 (130)	32 (0.96)	17 (2.3)	3.7 (0.64)

^a The values in parentheses are the sample standard deviations.^b Average and standard deviation values of two samples only that broke at clamp. ^c Except for one, all samples broke at clamp. Sample conditioned at 50% RH and 23 °C for one week (8.9% water).

water plasticizes the matrix and reduces MFC–matrix adhesion and perhaps also fibril–fibril bonding in the MFC network. Dufresne et al.³⁹ observed a similar effect of water on tunicin whisker/glycerol-plasticized starch composites. Another possible contribution is a higher modulus of the present wood-based MFC network. Reasons for this may include factors such as better nanofiber properties in wood-based MFC, better in-plane MFC alignment, and higher density of fibril–fibril bonds where moisture is likely to play a role.

The high performance of MFC networks containing only glycerol liquid is interesting (see Table 4). The strain-to-failure of 67 wt % MFC and 33 wt % glycerol is 9.3%, and the tensile strength is as high as 44 MPa. This illustrates the high load-bearing capacity of the network itself. In addition, the neat MFC film has fairly low strain-to-failure compared with that of glycerol-containing films. Glycerol likely plasticizes cellulose and thus contributes to higher toughness. This is supported by corresponding observations in our laboratory on the positive effect of RH on the strain-to-failure of neat MFC films.

At 60 wt % glycerol, the MFC network modulus is only 240 MPa. With 33 wt % glycerol as the matrix, the properties are much higher (2600 MPa) and similar to those of typical engineering polymers. The glycerol may interfere with the MFC network formation as reported elsewhere.^{31,39} This results in lower stiffness and strength. There is little difference in strain-to-failure for the 33 and 60 wt % glycerol matrix composites, thus supporting the idea that the MFC network itself controls this property. The effect of changes in the matrix glycerol content on nanocomposite properties is apparent in Table 4. As the glycerol content increases at a constant MFC content of 40 wt %, modulus and strength decrease. The strain-to-failure increases with glycerol content, but only to a certain limit because of the constraint from the MFC network.

For MFC/plasticized amylopectin composites with fixed matrix composition, increased MFC content leads to higher work of fracture. The highest value obtained (9.4 MJ/m³) is for 70 wt % MFC-plasticized amylopectin material. This can be compared with the value of the 100 wt % MFC film, 2.4 MJ/m³. Thus, the addition of plasticized amylopectin results in a highly toughened nanocomposite. Works of fracture for other materials are 1.0 MJ/m³ (steel), 3.0 MJ/m³ (bone), 10 MJ/m³ (natural rubber), 2.8 MJ/m³ (tendon), and 200 MJ/m³ (silk fibers).⁴⁸

Conclusions

An all-polysaccharide nanocomposite material with an MFC content as high as 70 wt % is successfully prepared and shows exceptionally high toughness (work of fracture). The starch matrix shows high compatibility with MFC, and this facilitates the uniquely high MFC content achieved. The material is bioinspired since it is based on renewable raw material sources, contains nanoscale cellulosic fibrils, has biodegradable characteristics, and, as in nature, the composites formation process takes place at ambient temperature and pressure with water as the medium. In addition, MFC disintegration is facilitated by enzymatic pretreatment of cellulose-rich wood fibers. The amorphous amylopectin matrix of the nanocomposite is highly plasticized in a 50/50 mixture of amylopectin and glycerol, thus mimicking the viscous character of the “matrix” in cellulose microfibril networks in plant cell walls. Microscopy studies reveal a layered nanocomposite structure and good MFC dispersion. A modulus of 6.2 GPa, a tensile strength as high as 160 MPa, and a strain-to-failure of 8.1% were observed at 70 wt % of MFC reinforcement. The work of fracture was as high as 9.4 MJ/m³. An important reason for this unique combination of strength and strain-to-failure in a viscous matrix composite is the nanoscale network structure of the MFC. It is a paper-like structure at a very fine scale and is also capable of large strain-to-failure at high fiber volume fractions. The nanostructured characteristics of MFC, in combination with favorable MFC–matrix adhesion, delay material damage during deformation and explain the observed ductility and high toughness. There was no sign of MFC-induced crystalline order in the amylopectin. Nanostructured MFC network reinforcement has the potential to substantially improve the properties of commercial starch-based materials such as films and foams.

Acknowledgment. The work was financed by the EU 6th framework IP “Sustainpack” project, and the Vinnova-Tekes Green materials programme (A.J.S.). In addition, the Biofibre Materials Centre and BioMime at KTH provided funding (M.A.S.A.S., L.B.). Lyckeby Stärkelsen is acknowledged for providing the amylopectin. The authors are grateful to Mikael Ankerfors and Professor Tom Lindström at STFI-Packforsk AB for the skilled preparation of MFC and discussions on the nature of MFC and MFC suspensions.

References and Notes

- (1) Eliasson, A.-C. *Starch in Food: Structure, Function and Applications*; Woodhead Publishing Limited: Cambridge, 2004.
- (2) Bastioli, C. Starch–polymer composites. In *Degradable Polymers*; Scott, G., Gilead, D., Eds.; Chapman & Hall: London, 1995.
- (3) Xiaofei, M.; Jiugao, Y. *Starch/Stärke* **2004**, *56*, 545.
- (4) Godbole, S.; Gote, S.; Latkar, M.; Chakrabarti, T. *Bioresour. Technol.* **2003**, *86*, 33.
- (5) Ke, T.; Sun, X. *J. Appl. Polym. Sci.* **2001**, *81*, 3069.
- (6) Matzinos, P.; Tserki, V.; Kontoyiannis, A.; Panayiotou, C. *Polym. Degrad. Stab.* **2002**, *77*, 17.
- (7) Xu, Y. X.; Kim, K. M.; Hanna, M. A.; Nag, D. *Ind. Crops Prod.* **2005**, *21*, 185.
- (8) Curvelo, A. A. S.; de Carvalho, A. J. F.; Agnelli, J. A. M. *Carbohydr. Polym.* **2001**, *45*, 183.
- (9) de Carvalho, A. J. F.; Curvelo, A. A. S.; Agnelli, J. A. M. *Int. J. Polym. Mater.* **2002**, *51*, 647.
- (10) de Carvalho, A. J. F.; Curvelo, A. A. S.; Agnelli, J. A. M. *Carbohydr. Polym.* **2001**, *45*, 189.
- (11) Chen, B.; Evans, J. R. G. *Carbohydr. Polym.* **2005**, *61*, 455.
- (12) Whitney, S. E. C.; Gothard, M. G. E.; Mitchell, J. T.; Gidley, M. J. *Plant Physiol.* **1999**, *121*, 657.
- (13) Herrick, F. W.; Casebier, R. L.; Hamilton, J. K.; Sandberg, K. R. *J. Appl. Polym. Sci.: Appl. Polym. Symp.* **1983**, *37*, 797.
- (14) Turbak, A. F.; Snyder, F. W.; Sandberg, K. R. *J. Appl. Polym. Sci.: Appl. Polym. Symp.* **1983**, *37*, 813.

- (15) Sakurada, I.; Nukushina, Y.; Ito, T. *J. Polym. Sci.* **1962**, 57, 651.
- (16) Wainwright, S. A.; Biggs, W. D.; Currey, J. D.; Gosline, J. M. *Mechanical Design in Organisms*; Princeton University Press: Princeton, NJ, 1982.
- (17) Brett, C. T.; Waldron, K. W. *Physiology and Biochemistry of Plant Cell Walls*, 2nd ed.; Chapman and Hall: London, 1996.
- (18) Henriksson, M.; Henriksson, G.; Berglund, L. A.; Lindström, T. *Eur. Polym. J.*, in press.
- (19) Berglund, L. A. Cellulose-based nanocomposites. In *Natural Fibers, Biopolymers and Biocomposites*; Mohanty, A. K., Misra, M., Drzal, L. T., Eds.; CRC Press: Boca Raton, FL, 2005.
- (20) Azizi Samir, M. A. S.; Alloin, F.; Dufresne, A. *Biomacromolecules* **2005**, 6, 612.
- (21) Boldizar, A.; Klason, C.; Kubát, J.; Näslund, P.; Sáha, P. *Int. J. Polym. Mater.* **1987**, 11, 229.
- (22) Favier, V.; Chanzy, H.; Cavaillé, J. Y. *Macromolecules* **1995**, 28, 6365.
- (23) Favier, V.; Canova, G. R.; Cavaillé, J. Y.; Chanzy, H.; Dufresne, A.; Gauthier, C. *Polym. Adv. Technol.* **1995**, 6, 351.
- (24) Iguchi, M.; Yamanaka, S.; Budhiono, A. *J. Mater. Sci.* **2000**, 35, 261.
- (25) Nakagaito A. N.; Yano, H. *Appl. Phys. A: Mater. Sci. Process.* **2005**, 80, 155.
- (26) Yano, H.; Nakahara, S. *J. Mater. Sci.* **2004**, 39, 1635.
- (27) Dufresne, A.; Dupeyre, D.; Vignon, M. R. *J. Appl. Polym. Sci.* **2000**, 76, 2080.
- (28) López-Rubio, A.; Lagaron, J. M.; Ankerfors, M.; Lindström, T.; Nordqvist, D.; Mattozzi, A.; Hedenqvist, M. S. *Carbohydr. Polym.* **2007**, 68, 718.
- (29) Pääkkö, M.; Ankerfors, M.; Kosonen, H.; Nykänen, A.; Ahola, S.; Österberg, M.; Ruokolainen, J.; Laine, J.; Larsson, T.; Ikkala, O.; Lindström, T. *Biomacromolecules*, in press.
- (30) Baggerud, E.; Stenström, S.; Lindström, T. Measurement of volume fractions of solid, liquid and gas in kraft and CTMP paper at varying moisture content. In *Proceedings of the International Paper Physics Conference*; TAPPI Press: Atlanta, GA, 2003; pp 157–163.
- (31) Anglès, M. N.; Dufresne, A. *Macromolecules* **2000**, 33, 8344.
- (32) Forssell, P. M.; Mikkilä, J. M.; Moates, G. K.; Parker, R. *Carbohydr. Polym.* **1997**, 34, 275.
- (33) Moates, G. K.; Noel, T. R.; Parker, R.; Ring, S. G. *Carbohydr. Polym.* **2001**, 44, 247.
- (34) Agarwal, B. D.; Broutman, L. J. *Analysis and Performance of Fiber Composites*; John Wiley & Sons: New York, 1990.
- (35) Ardizzone, S.; Dioguardi, F. S.; Mussini, T.; Mussini, P. R.; Rondinini, S.; Vercelli, B.; Vertova, A. *Cellulose* **1999**, 6, 57.
- (36) Helbert, W.; Chanzy, H. *Carbohydr. Polym.* **1994**, 24, 199.
- (37) Rindlav-Westling, A.; Stading, M.; Hermansson, A.-M.; Gatenholm, P. *Carbohydr. Polym.* **1998**, 36, 217.
- (38) Lu, Y.; Weng, L.; Cao, X. *Carbohydr. Polym.* **2006**, 63, 198.
- (39) Anglès, M. N.; Dufresne, A. *Macromolecules* **2001**, 34, 2921.
- (40) Gopalan Nair, K.; Dufresne, A. *Biomacromolecules* **2003**, 4, 657.
- (41) Gopalan Nair, K.; Dufresne, A. *Biomacromolecules* **2003**, 4, 666.
- (42) Gopalan Nair, K.; Dufresne, A.; Gandini A.; Belgacem M. N. *Biomacromolecules* **2003**, 4, 1835.
- (43) Butler, M. F.; Cameron, R. E. *Polymer* **2000**, 41, 2249.
- (44) Montès, H.; Mazeau, K.; Cavaillé, J. Y. *J. Non-Cryst. Solids* **1998**, 235–237, 416.
- (45) Montès, H.; Mazeau, K.; Cavaillé, J. Y. *Macromolecules* **1997**, 30, 6977.
- (46) Hull, D. *An Introduction to Composite Materials*; Cambridge University Press: Cambridge, 1981.
- (47) Ota, W. N.; Amico, S. C.; Satyanarayana, K. G. *Compos. Sci. Technol.* **2005**, 65, 873.
- (48) Vogel, S. *Comparative Biomechanics: Life's Physical World*; Princeton University Press: Princeton, NJ, 2003.

BM0703160